Supporting Information

Experimental Section

SURMOF synthesis: The $Cu_2(F_2AzoBDC)_2(dabco)$ SURMOF thin films were prepared in a layer-by-layer fashion directly on the substrate. The substrates are gold-coated silicon wafer surfaces functionalized with an 11-mercapto-1-undecanol self-assembled monolayer (MUD SAM). The layer-by-layer growth process consists of alternately immersing the substrate in the ethanolic solutions of the MOF components, which are the copper acetate metal nodes (15 min) and the organic linker molecules (30 min), which are dabco (1,4-diazabicyclo[2.2.2]octane) and F_2AzoBDC ((*E*)-2-((2,6-difluorophenyl)diazenyl)terephthalic acid). The concentrations are 1 mM for the metal nodes and 0.2 mM for the organic components. The samples were cleaned with pure ethanol for 2 min between each immersion step. The synthesis was performed with a dipping robot.[1] The first 10 cycles were performed at a temperature 50°C, the following 190 cycles at room temperature. The samples were prepared in 200 cycles in total.

SURMOF pore loading with 1,4-butanediol, hexadecane and 2-octanol: The guest molecules loadings of the SURMOF films were performed from the gas/vapor phase. A glass bottle (50 mL) was filled with Raschig-rings (10 mm × 10 mm, soda-lime glass) in the bottom part of the bottle to obtain an elevated flat platform for the sample. 1,4-butanediol, hexadecane or 2-octanol (5 mL each) was filled into the bottom of the bottle. The sample was placed on top of the Raschig-rings for vapor loading at room temperature (298 K). Before the loading, the sample was activated under vacuum overnight to remove residual solvent molecules from the pores. For almost saturated vapor, the uptake of 1,4-butanediol by $Cu_2(F_2AzoBDC)_2(dabco)$ SURMOF was quantified using a quartz crystal microbalance and an average loading of 1/3 butanediol molecule per unit cell was found.[2] The transient uptake is measured with a quartz crystal microbalance (QCM).

X-ray diffraction (XRD): The X-ray diffractograms were measured in out-of-plane geometry using a Bruker D8-Advance diffractometer equipped with a position-sensitive detector in Θ–2Θ geometry. A Cu-anode causing X-ray with a wavelength of $\lambda = 0.154$ nm was used. The measurements were carried out within a range of $2\theta = 3°$-20° with a step width of 0.02°. The in-plane XRD data were measured using a Bruker D8 Discover diffractometer with a wavelength of $\lambda = 0.154$ nm, equipped additionally with a tilt-stage, a quarter Eulerian cradle and 2.3° Sollar-slits. The measurements were carried out within $2\theta = 3°$-20° with a step width of 0.02°.

Scanning electron microscopy and energy-dispersive X-ray: The scanning electron microscope (SEM) and energy-dispersive X-ray (EDX) measurements were performed on a TESCAN VEGA3 thermionic emission SEM system equipped with a Bruker EDX unit. For the cross-section analysis, the samples were broken. In order to avoid charging effects, all samples were coated with a 3~4 nm thick platinum film by sputtering at high vacuum before recording the SEM images and EDX spectra.

Infrared reflection absorption spectroscopy: The infrared reflection absorption (IRRA) spectra on thin films were recorded at a Bruker Vertex 80, using a resolution of 2 cm^{-1}. All measurements were performed in grazing incidence reflection mode at an angle of incidence of 80° relative to the surface normal.

Quartz crystal microbalance measurements: The QSense E4 quartz crystal microbalance with dissipation (QCM-D) was used to measure the uptakes of guest molecules including 1,4-butanediol, 2-octanol and hexadecane at a resonance frequency of approximately 5 MHz. The QCM cell was connected to the nitrogen flow system. Before each measurement, the sample was activated in pure nitrogen flow at 65°C overnight to reach a stable baseline and empty the SURMOF pores. Then the measurement was performed at 25°C.

For the photoswitching, the samples were irradiated with light from LEDs from PrizMatix. Green light with a wavelength of 530 nm and an intensity of roughly 10 mW/cm^2 annd violet light of 400 nm wavelength and an intensity of roughly15 mW/cm^2. The irradiation time was 30 min. The irradiation was performed at room temperature in common air.

The *trans* state is thermodynamically stable in the dark. The *cis* state is metastable and slowly isomerizes to the *trans* state. At room temperature, the time constant to the *cis*-to-*trans* relaxation is approximately 2 years at room temperature.[20, 21]

Atomic force microscopy: The atomic force microscope (AFM) measurements were performed on Bruker Dimension® Icon™ SPM system in tapping quantitative nanomechanical (QNM) mode in air. The cantilever was used NSC18/Cr-Au_BS type (2.8 N/m). Both of the measurements were carried out with 512 scan lines in 0.2 Hz scan rate. The scan position was marked by an artificial scratch.

Contact Angle Measurements: Static contact angles (CA) were measured with an *attension* optical contact angle analysis systems from Biolin Scientific. The experiments were performed under ambient conditions at 23.0°C and a humidity of about 44%. The contact angles were obtained by depositing droplets of 2 µL of deionized water on the sample surface using a micro syringe, while recording the images. The image analysis was carried out with the software "*one attension*" using a Young-Laplace analysis mode and an air-to-H_2O interface. Three measurements were performed at different pristine positions on each surface and contact angle data were recorded from three distinct samples. The resulting contact angles were averaged and the standard deviation is shown as error bars in Figures 3 and 4.

Author contributions

ZZ performed the syntheses, the experiments (except of AFM) and analyzed the data. DC performed the AFM experiments. DM and SH synthesized the custom-made MOF linker. LH designed the project. ZZ and LH wrote the manuscript, approved by all authors.

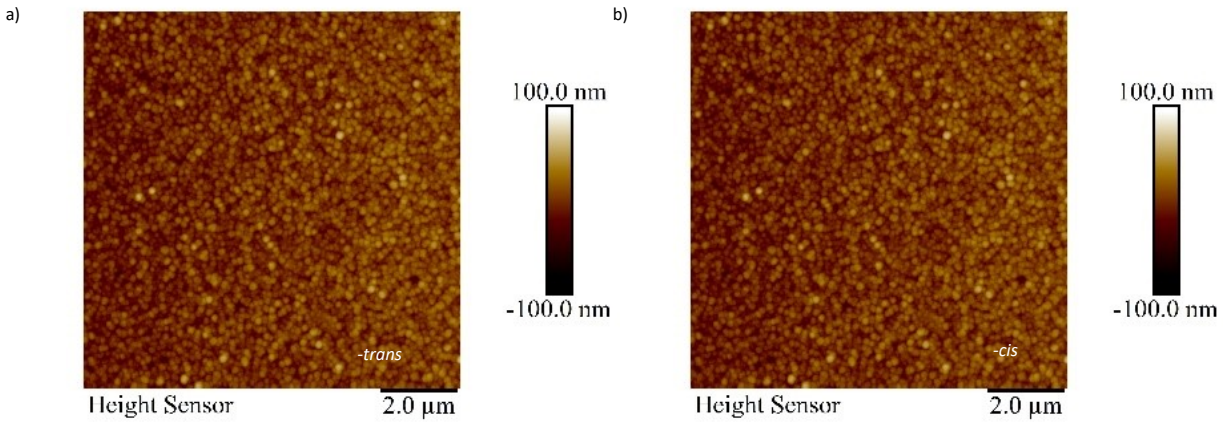

Figure S1. Atomic force microscopy images of the $Cu_2(F_2AzoBDC)_2(dabco)$ SURMOF films in the **a)** *trans* and **b)** *cis* state. The imaging of the sample was performed at the same position. After imaging the sample in the *trans* state (a), the sample was irradiated with green light for 30 min, before recording the image b).

The surface roughness (i.e. the root-mean square roughness, Rq) in *trans* is 12.7 nm (a) and in *cis* is 12.8 nm (b). The arithmetic average roughness (Ra) values are 10.0 nm in *trans* and 10.2 nm in *cis*.

As result, no changes in the morphology and of the roughness are observed when switching the SURMOF from *trans* to *cis*. (Please note, small deviations between subsequent AFM images are usually unavoidable.)

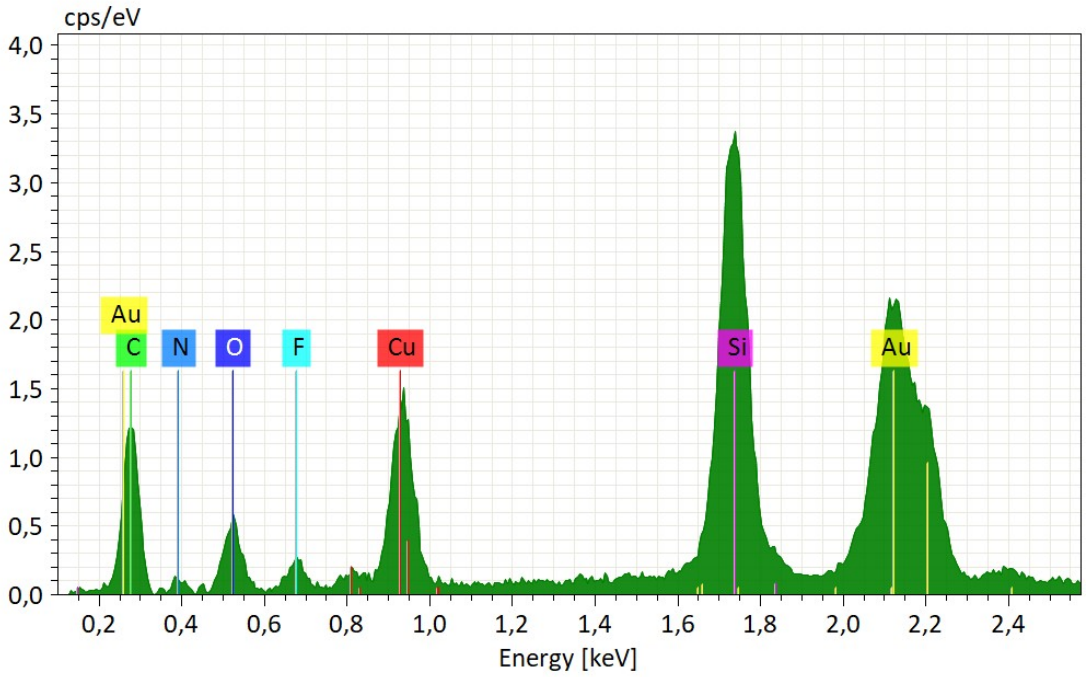

Figure S2. Energy-dispersive X-ray spectroscopy of the $Cu_2(F_2AzoBDC)_2(dabco)$ SURMOF films. The peaks are assigned to the atoms. In the EDX spectroscopy, the relative atomic amounts of C, N, O, F and Cu are determined, table S1. The atomic ratios of nitrogen and fluorine versus copper determined by EDX are in good agreement with the ratios following from the $Cu_2(F_2AzoBDC)_2(dabco)$ structure. (We focus in the analysis of N, F and Cu, which can be found in the SURMOF but not in the substrate.)

Table S1. EDX data of the $Cu_2(F_2AzoBDC)_2(dabco)$ SURMOF films.

	Cu:N	Cu:F
Atomic ratio in ideal $Cu_2(F_2AzoBDC)_2(dabco)$ / %	1 : 3	1 : 2
Atomic ratio determined by EDX / %	1 : 2.88	1 : 2.07

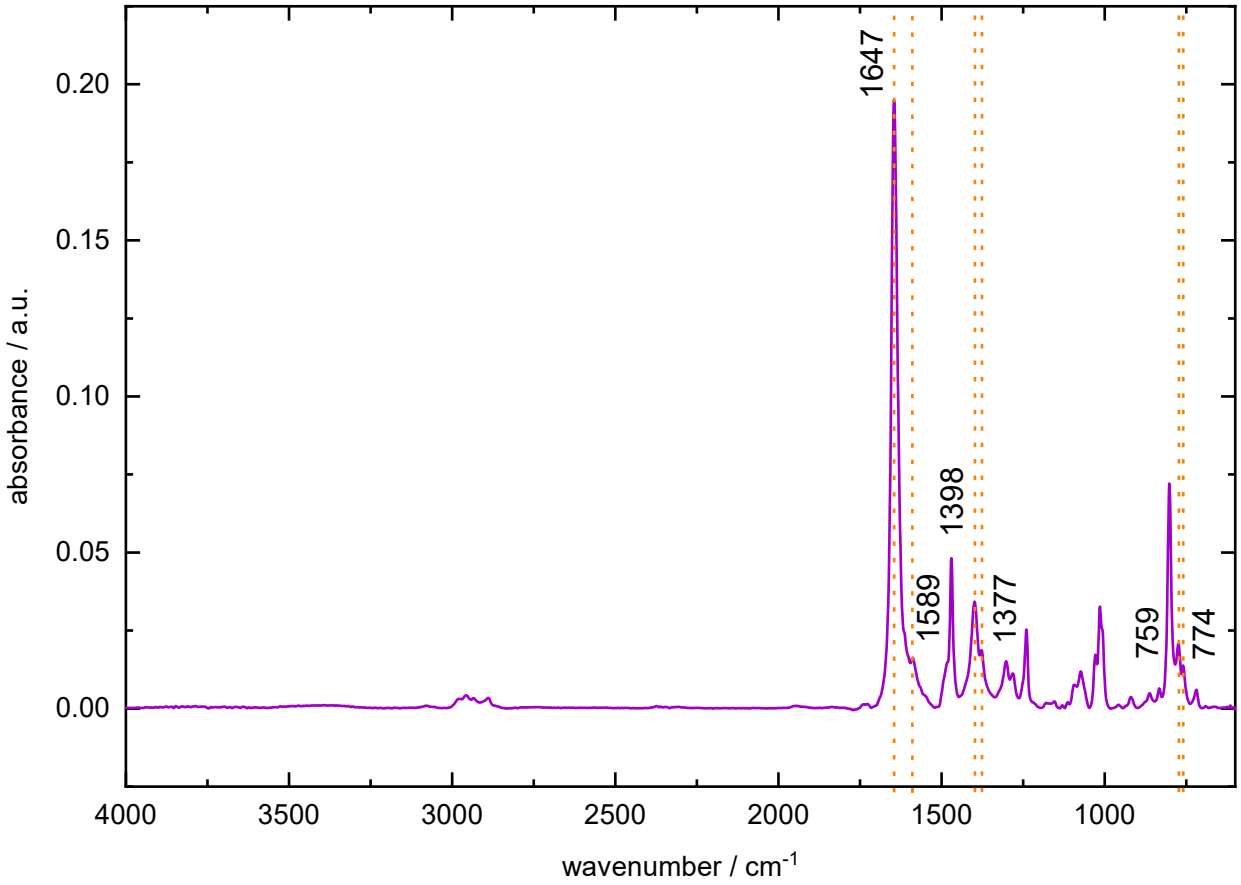

Figure S3. Infrared reflection absorption spectroscopy (IRRAS) of the *trans* $Cu_2(F_2AzoBDC)_2(dabco)$ SURMOF films. The vibration bands at 774cm^{-1}, 1377cm^{-1} and 1398cm^{-1} are assigned to the fluorinated azobenzene.[3] The vibration bands at 759 cm^{-1}, 1589 cm^{-1} and 1647 cm^{-1} are assigned to Ph-H bending, C=C and O-C=O stretch vibrations, respectively, of the MOF linkers.[4-6] Strong vibration bands caused by a significant defect density in the MOF,[7] are not observed.

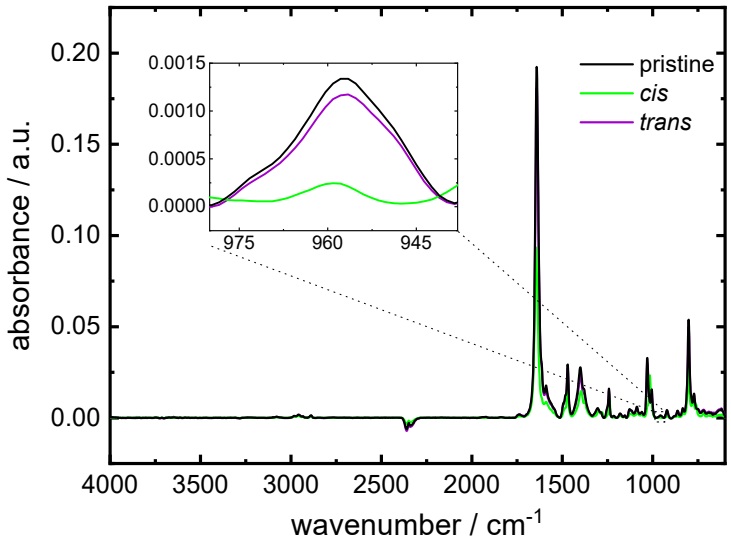

Figure S4. Infrared reflection absorption spectra of the $Cu_2(F_2AzoBDC)_2(dabco)$ SURMOF films. The thermally relaxed sample (100% *trans*) is labeled as pristine (black). The sample upon irradiation with violet and green light is shown in violet and green, respectively. The zoom-in of the *trans*-azobenzene vibration band at 957 cm^{-1} is shown. The array of the band decreases to 14% of the pristine value upon green light and 86% upon violet light. Based on this, the photostationary state (PSS) was determined. Upon irradiation with green light, a PSS of 16% *trans* (and 84% *cis*, referred to as *cis* state) was determined. Upon irradiation with violet light of 400 nm, 85% *trans* (and 15% *cis*, referred to as *trans* state) was determined.

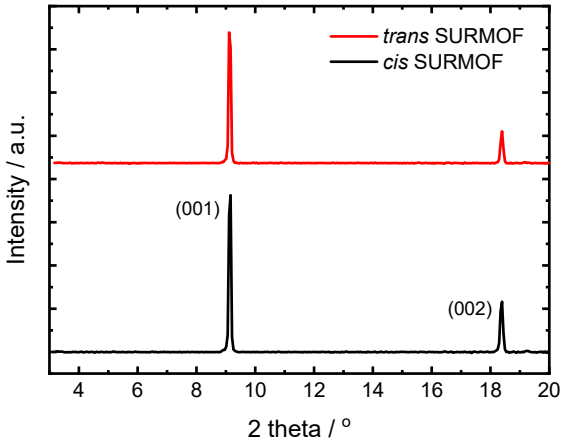

Figure S5. X-ray diffractograms (XRDs) of $Cu_2(F_2AzoBDC)_2(dabco)$ SURMOF films in the *trans* and *cis* state, see labels. The peak positions are not affected by the azobenzene photoswitching. A small shift of the XRD-form-factor as result of the *trans-cis* switching can be observed from the change of the relative intensities of the (001) and (002) peaks.

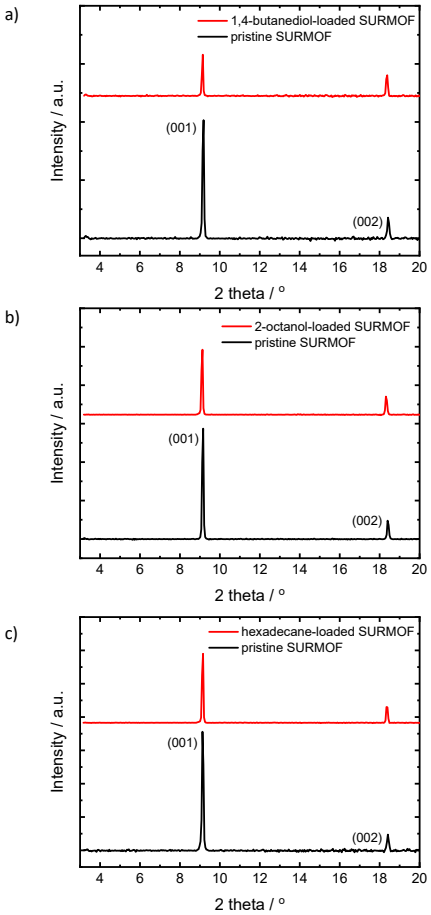

Figure S6. X-ray diffractograms (XRDs) of $Cu_2(F_2AzoBDC)_2(dabco)$ SURMOF films before and after loading with a) 1,4-butanediol, b) 2-octanol and c) hexadecane, respectively. The peak positions are not affected by the guest loading, indicating that the SURMOF structure is not modified by the guest loading. The intensity ratios (001):(002) decrease from 5.7 to 2.0, from 6.0 to 3.6 and from 7.5 to 4.3 after loading with 1,4-butanediol, 2-octanol and hexadecane, respectively. This indicates a modification of the XRD form factor as result of the guest loading, verifying the guest-loading in the pores.

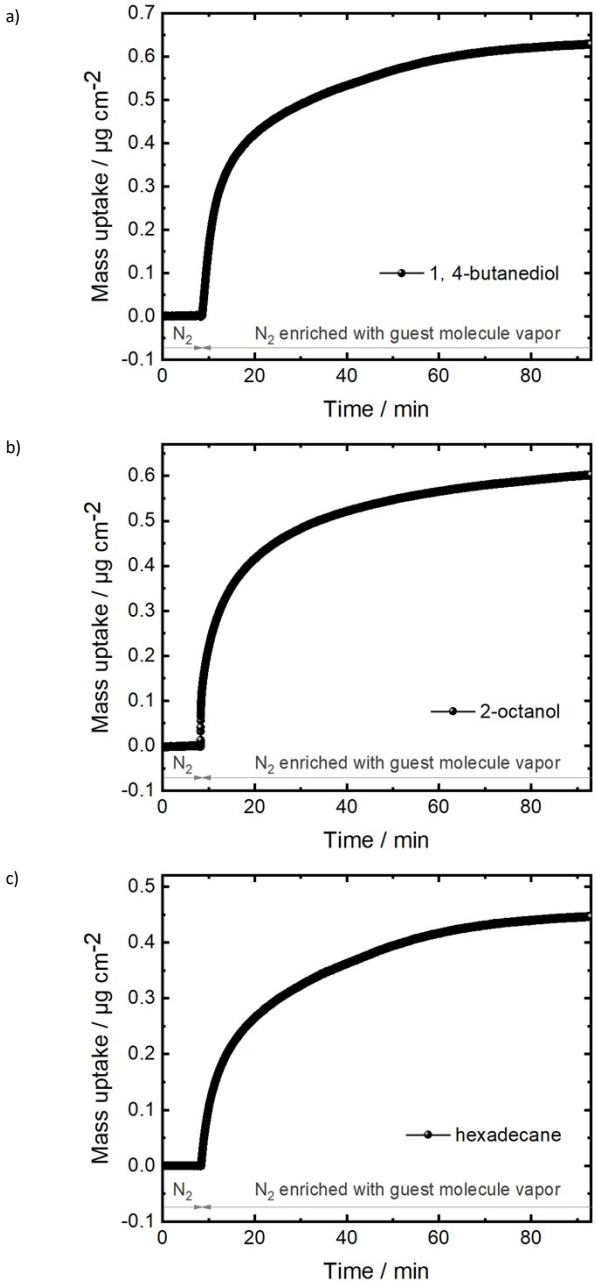

Figure S7. Uptakes of **a)** 1,4-butanediol, **b)** 2-octanol and **c)** hexadecane by the $Cu_2(F_2AzoBDC)_2(dabco)$ SURMOF films. The uptake as a function of time was measured with a quartz crystal microbalance. The data show that the guest molecules can be embedded in the SURMOF pores.
The samples were prepared in 50 synthesis cycles using the dipping robot. (There, the SURMOF-mass-increase during the synthesis cannot be determined. Thus, the molecular loading in units like molecules per unit cell cannot be calculated.)

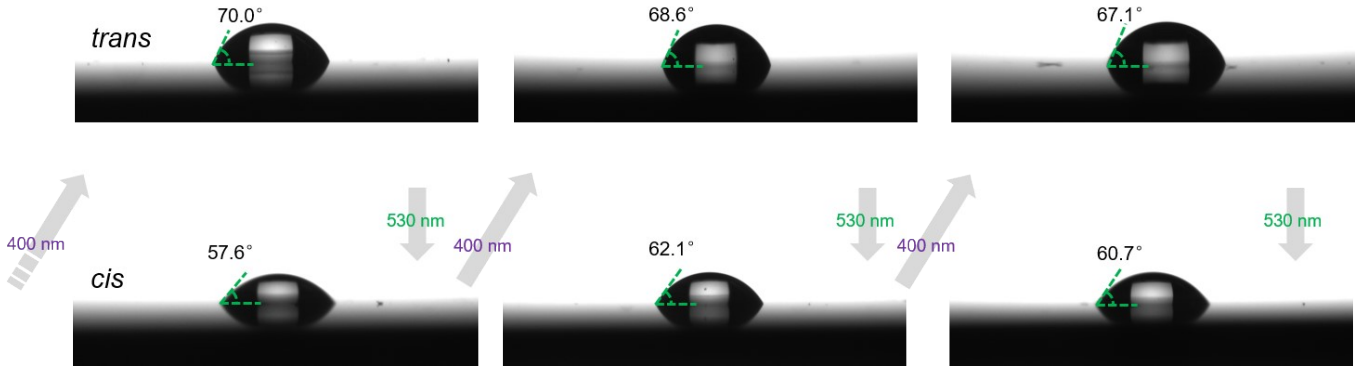

Figure S8. The contact angle images with a water droplet on the $Cu_2(F_2AzoBDC)_2(dabco)$ SURMOF film. The SURMOF film was **unloaded.** The sample states (*trans* or *cis*) are labelled. Three *trans*-*cis*-photoswitching cycles were performed.

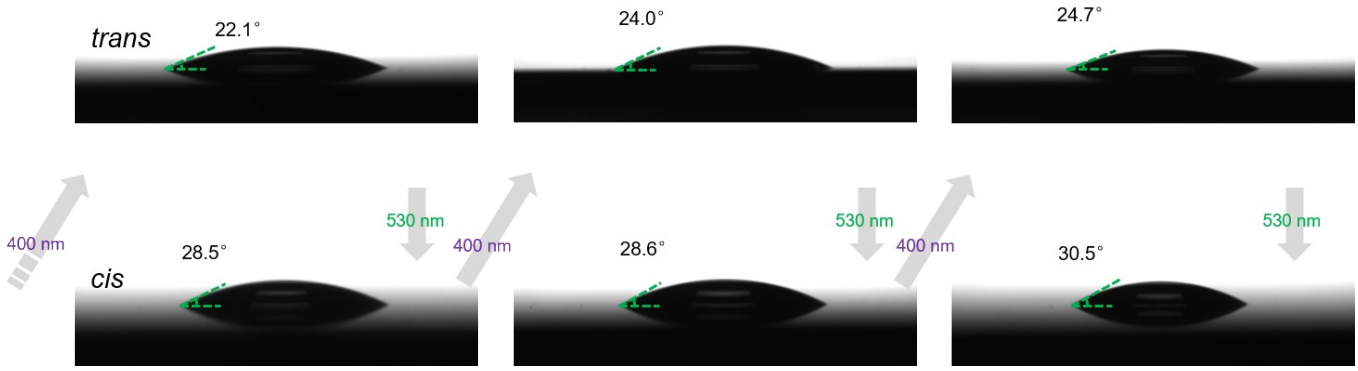

Figure S9. The contact angle images with a water droplet on the $Cu_2(F_2AzoBDC)_2(dabco)$ SURMOF film. The SURMOF film was **loaded with 1,4-butanediol**. The sample states (*trans* or *cis*) are labelled. Three *trans*-*cis*-photoswitching cycles were performed.

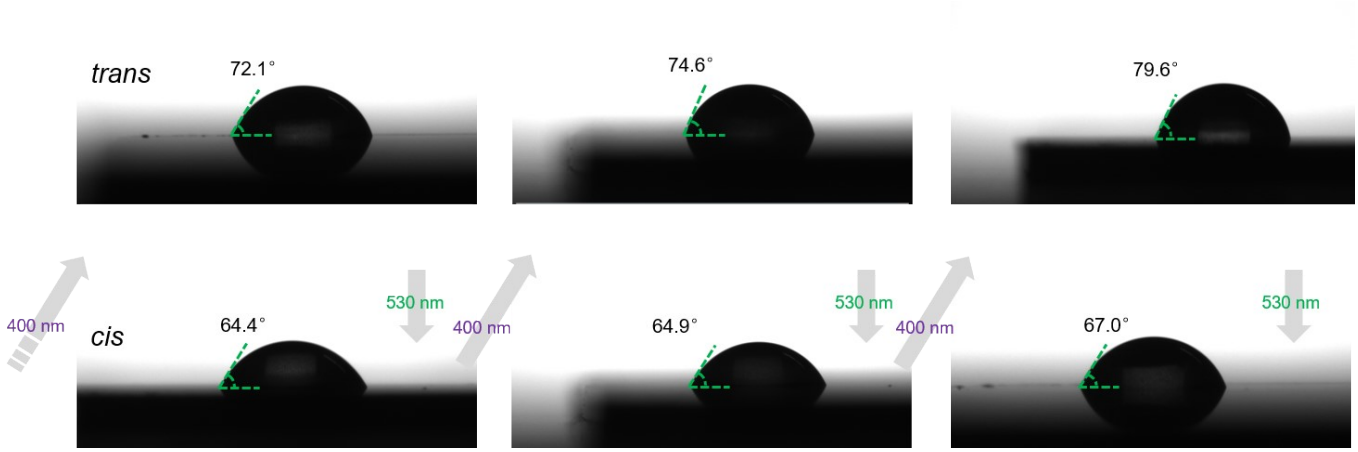

Figure S10. The contact angle images with a water droplet on the $Cu_2(F_2AzoBDC)_2(dabco)$ SURMOF film. The SURMOF film was **loaded with 2-octanol**. The sample states (*trans* or *cis*) are labelled. Three *trans*-*cis*-photoswitching cycles were performed.

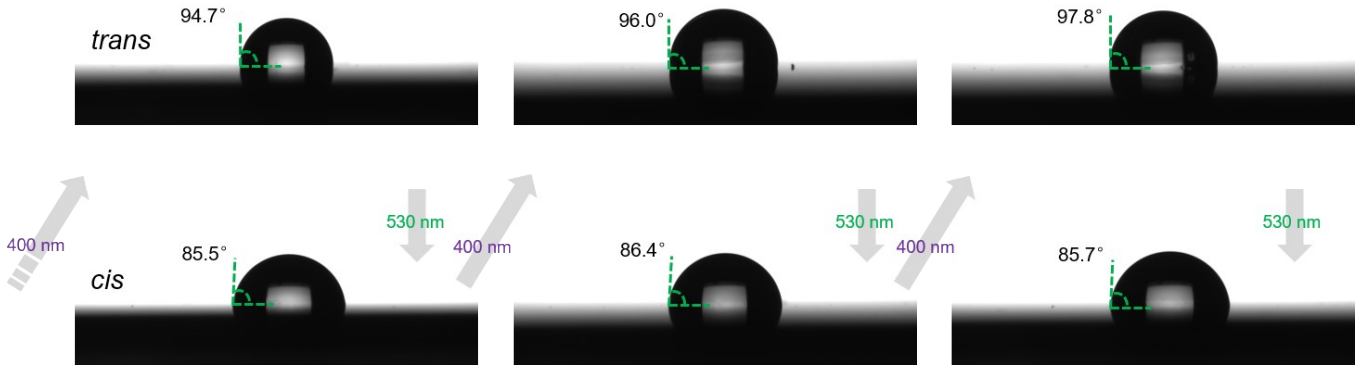

Figure S11. The contact angle images with a water droplet on the $Cu_2(F_2AzoBDC)_2(dabco)$ SURMOF film. The SURMOF film was **loaded with hexadecane**. The sample states (*trans* or *cis*) are labelled. Three *trans*-*cis*-photoswitching cycles were performed.

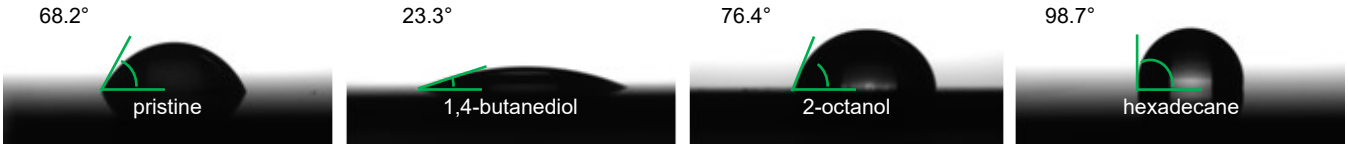

Figure S12. Photographs and contact angles of the water droplet on the same sample: pristine → after loading with 1,4-butanediol → 2-octanol → hexadecane (left to right; see labels).

.

References

1. Z.-G. Gu, A. Pfriem, S. Hamsch, H. Breitwieser, J. Wohlgemuth, L. Heinke*, H. Gliemann and C. Wöll, *Microporous Mesoporous Mater.*, 2015, **211**, 82-87.
2. K. Müller, J. Helfferich, F. L. Zhao, R. Verma, A. B. Kanj, V. Meded, D. Bléger, W. Wenzel and L. Heinke, *Adv. Mater.*, 2018, **30**, 1706551
3. Q. Yi and G. B. Sukhorukov, *Soft Matter*, 2014, **10**, 1384-1391.
4. O. Zybaylo, O. Shekhah, H. Wang, M. Tafipolsky, R. Schmid, D. Johannsmann and C. Wöll, *Phys. Chem. Chem. Phys.*, 2010, **12**, 8093-8098.
5. H. Jacob, S. Ulrich, U. Jung, S. Lemke, T. Rusch, C. Schütt, F. Petersen, T. Strunskus, O. Magnussen, R. Herges and F. Tuczek, *Phys. Chem. Chem. Phys.*, 2014, **16**, 22643-22650.
6. P. F. Driscoll, N. Purohit, N. Wanichacheva, C. R. Lambert and W. G. McGimpsey, *Langmuir*, 2007, **23**, 13181-13187.
7. K. Müller, N. Vankova, L. Schottner, T. Heine and L. Heinke, *Chem. Sci.*, 2019, **10**, 153-160.